

6.8 Summary and conclusions

A general model for multiple precipitation reactions in multicomponent systems has been created using the thermodynamic software MT-DATA as part of a FORTRAN program. Effects particular to multicomponent systems have been shown to have significant importance and have been accounted for. This includes a treatment of the flux-balance problem and of multicomponent capillarity.

A major difficulty remains in the lack of reliable quantitative experimental data. However, general semi-quantitative aspects are very well predicted considering the relative simplicity of the model, which, for example, does not account for the role of grain boundaries. This causes an over estimation of the overall growth rate, as the actual hard impingement effects are underestimated for phases growing on grain boundaries.

A further effect of the multicomponent nature of the systems considered appeared in the calculation of the nucleation rate. It was shown that examining the nucleation rates in terms of driving force only, could lead to considerable error. An argument was proposed to explain that the prefactor N in the classical nucleation theory was itself strongly dependent on the composition. This implies the existence of strong limitations in the predictive power of any model based on the classical theory for nucleation, as the value of N may have to be fitted for each single composition. It seems important to reconsider the classical theory for nucleation and adapt it so as to deal with multicomponent effects.

Chapter 7

Experimental Procedures

7.1 Introduction

The experimental work consists essentially of the identification of different kinds of precipitates formed during ageing treatments.

As has been outlined in the presentation of precipitated phases in austenitic stainless steels, the identification of carbides, nitrides and intermetallic phases is not straightforward, bearing in mind that:

- The size of the precipitates ranges from about 15 nm to 5 μm . For the smallest particles, only TEM (transmission electron microscopy) is appropriate, but it is not for the largest as very few are likely to be found in the observable area of a thin foil. The larger particles are also not expected on carbon replicas, because the film is not strong enough to hold them. Diffraction patterns are also difficult to obtain from large particles.
- Some precipitates have similar crystal structures and lattice parameters (e.g. $M_{23}C_6$, M_6C , G-phase). Therefore, any technique which relies solely on structure determination is susceptible to error.
- Some precipitates have similar compositions, so that ‘fingerprinting techniques’ based on microanalysis can be ambiguous when used on their own.

It clearly is necessary to use complementary techniques. The experimental procedure is depicted in figure 7.1.

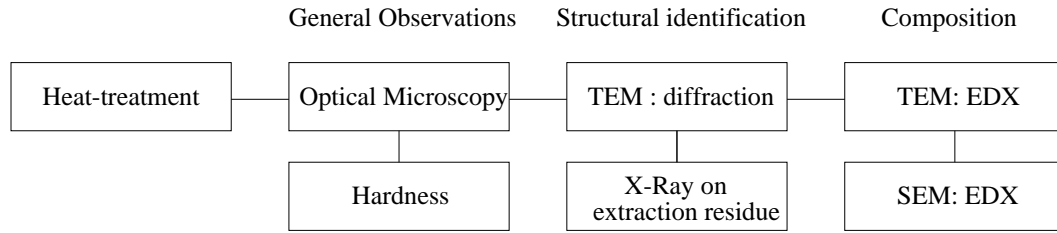


Figure 7.1: Complementary techniques used for identification of precipitates and general observations of ageing effects. TEM: transmission electron microscopy. EDX: energy dispersive X-ray analysis. SEM: scanning electron microscopy.

7.2 Materials and heat-treatments

Two steels were provided by National Power: NF709, and a variant called NF709R (both manufactured by Nippon Steel). NF709, based on 20/25 austenitic stainless steels, has been designed recently and is regarded as the best creep resistant austenitic stainless steel available today. The chemical compositions are given in table 7.1. The steels were

NF709 wt%	Cr	Ni	Mn	Mo	Si	Nb	Ti	N	C	B	P
	20.28	24.95	1.00	1.50	0.41	0.26	0.05	0.167	0.06	0.005	0.006
NF709R wt%	Cr	Ni	Mn	Mo	Si	Nb	Ti	N	C	B	P
	22.22	25.34	0.92	1.40	0.38	0.24	0.05	0.170	0.03	0.005	0.022

Table 7.1: Composition of steels studied. NF709R is a variant of the first steel provided, NF709, with increased Cr and reduced C.

received in the form of tubes from which two kinds of specimens were made. Rods of 3 mm in diameter and various lengths were machined; they were used to prepare thin foils. Sections of the tubes were cut so as to provide samples for replication, optical microscopy, hardness, *etc...* (figure 7.2). The grain size was smaller along the inner and outer walls of the tubes. The longitudinal sections were made carefully so as to cross the tube and present some regions from the outer wall and the middle of the tube wall.

Pairs of each kind (rod and piece) of sample were sealed in silica tubes under a pressure of argon of about 0.1 atm. They were water quenched at the end of the heat-treatment.

Both NF709 and NF709R were aged at 750 °C and 800 °C for up to 15000 h.

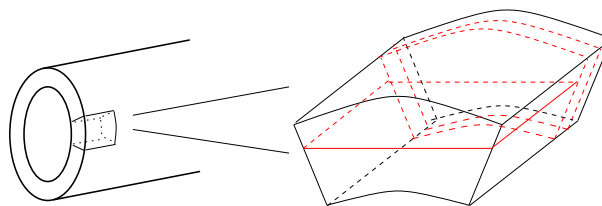


Figure 7.2: Preparation of specimen from received tubes. Longitudinal sections were used for SEM and preparation of replicas, transverse sections for optical microscopy and hardness. The samples are typically 1 cm long and 5 mm thick.

7.3 Optical microscopy

The specimens for optical microscopy were hot mounted with conductive bakelite powder, ground with silicon carbide paper down to 1200 grit and then polished with 6 and 1 μm diamond paste. Electrolytic etching was done in a solution of 10% oxalic acid in distilled water, at about 5 V. This electrolyte attacks the precipitates and σ -phase, but not the matrix. Grain boundaries are only revealed after about 60 s when they are precipitate free.

Using a solution of 10% HCl in methanol also gave satisfying results (6 V for 10 to 30 s). This electrolyte attacks the matrix but not the precipitates.

A selective etchant was also used to reveal σ -phase. The samples were electrolytically etched (5 to 10 s at 1.5-3 V) in a solution of 56 g KOH for 100 ml of water. This colours σ -phase brown.

Optical microscopy gives a general impression of the amount of precipitates and on their locations (grain boundary, twin boundary, intragranular). Phases such as grain-boundary σ -phase can be identified readily.

7.4 X-ray analysis of extraction residues

Each kind of precipitate makes only $< 1\%$ in volume of the bulk sample. For this reason, X-ray diffraction on a bulk specimen is unlikely to provide accurate information about precipitates. A method commonly used to avoid this difficulty involves the electrolytic dissolution of the matrix, leaving residues which can be analysed by X-ray diffraction.

Details of the experimental settings are shown in figure 7.3, together with a typical

X-ray spectrum of extracted residues. Specimens of a few hundred milligrammes were

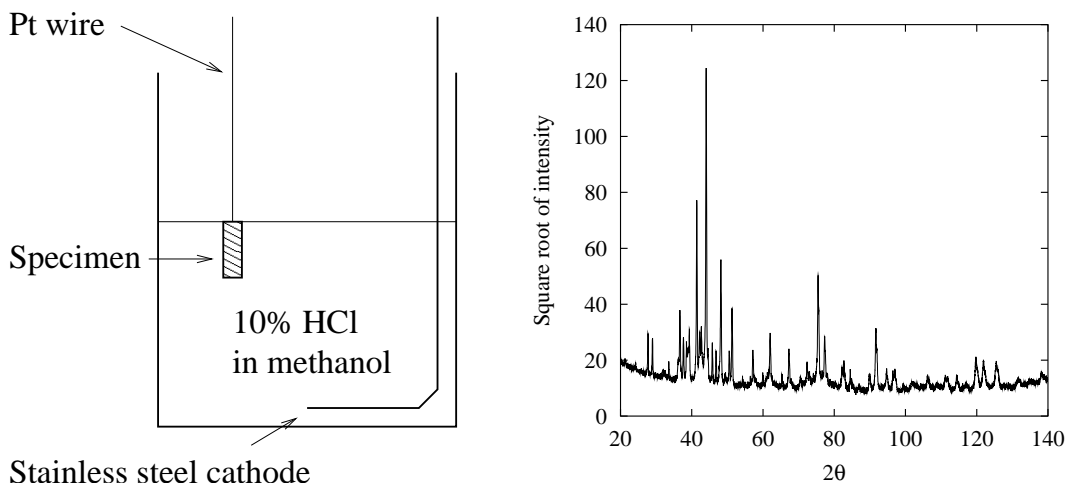


Figure 7.3: The experimental settings used to electrolytically dissolve samples of NF709. A typical X-ray spectrum of extracted residues is illustrated on the right.

dissolved electrolytically in a solution of 10% HCl in methanol. The ensemble made by the platinum wire and the specimen (figure 7.3) was weighed before and after dissolution, with a precision balance, so as to provide an estimate of the amount of steel dissolved. The residues were filtered using a $0.2 \mu\text{m}$ membrane filter (filtering using a $0.1 \mu\text{m}$ was not possible within a reasonable amount of time). The filter was then allowed to dry for one day. It was weighed before and after filtration, so as to measure the amount of residue collected.

The filter was then placed in a 2θ X-ray diffractometer. Identification of the different phases was often made difficult because of the overlapping of many peaks. An analysis was also performed on the filter by itself in order to remove any peak coming from it.

This technique is very useful when used in conjunction with other identification methods. The main advantages are that it should reveal all of the precipitates present, that the amount of material investigated at once is far greater than with most of the other methods (scanning electron microscopy, transmission EM, *etc...*) and that it can give, in principle, quantitative information. It is also relatively easy to implement when compared to methods such as TEM for which the sample preparation can be much more time consuming.

The disadvantages are that no information are obtained about the morphology, distribution or location of the precipitates. In practice, quantitative information can only be

obtained if the absorption coefficients (μ) or their ratio (μ/μ_{cor}) to a that of a reference phase (corundum) are known, which was not the case for most of the phases found in the present work. Another limitation concerns the size of the precipitates. Comparison with the phases detected with this method and those found using TEM show that the smallest precipitates are most probably dissolved.

7.5 Transmission electron microscopy

This is by far the most important experimental method in this project justifying a more detailed presentation of specimen preparation and precipitate identification.

7.5.a Preparation of samples

i Carbon replicas

Carbon replicas were prepared on samples mounted in the same way as for metallographic specimens. At first, the polished surface was lightly etched with a 10% HCl in methanol solution, which attacks the matrix but not the carbides (oxalic acid cannot be used as it attacks the carbides but not the matrix).

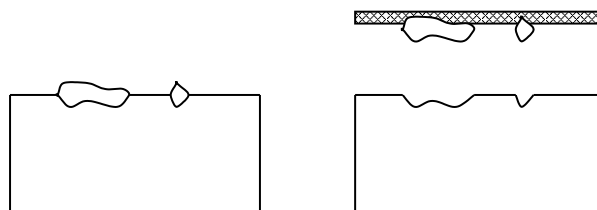


Figure 7.4: Preparation of carbon replicas. On the left a schematic drawing of the etched sample. On the right, the carbon film has extracted the precipitates

A carbon film was then applied on the surface using a vacuum vaporising system. The thickness of the film is a critical factor: too thin and it will be destroyed by the electron beam. By contrast, a thick film is difficult if not impossible to lift. The film was cut on the surface into small squares, the specimen was electrolytically etched in the same solution, rinsed in methanol and then in distilled water. The pieces of film were collected on 3 mm diameter copper grids. For specimens aged over long periods of time (2500 h and more), it became increasingly difficult to obtain nice replicas. This was attributed to the density of precipitation and the presence of very large particles on the grain boundaries.

Carbon replicas offer a much larger observable area than thin foils, but it is more difficult to tilt to a major zone axis, because of the very small size of the diffracting particle. Also, it is possible that some particles are not extracted.

ii Preparation of thin foils

Thin foils were cut from the 3 mm rods to about 100 μm , then ground with silicon carbide paper (1200 grit) on both sides, until the thickness was about 50 μm . Care was taken to avoid deformation which can cause the formation of martensite.

The foils were then electropolished using a twin-jet electropolisher initially with a solution of 5% perchloric acid, 15% glycerol in 80% methanol. Although some thin foils were satisfactory, the repeatability was low and another solution was used, made of 5% perchloric acid in 2n-ethoxy-butanol, which gave more satisfying results.

Although thin foils offer a much smaller observable area, the presence of the austenitic matrix greatly simplifies tilting as it is possible to take advantage of the orientation relationships which often exist between it and the variety of precipitates.

7.5.b Identification of precipitates with TEM

Two microscopes were used for this work, a Philips CM30 capable of acceleration tensions of 300 kV, and a JEOL 2000FX (200 kV). Both were fitted with an energy dispersive X-ray analysis (EDX) facility and an electron energy loss spectrometer (EELS). Therefore both structure and chemical composition could be investigated.

i Structure identification: electron diffraction

Conventional selected-area diffraction and convergent beam electron diffraction techniques were used. The latter was required to identify independently small precipitates on carbon replicas; it was also useful when tilting the sample to a major zone axis. A schematic drawing of both techniques is found in figure 7.5. In conventional diffraction, the distance between two different spots in the pattern (R_{hkl}) is related to the spacing d_{hkl} for the planes of Bragg indices hkl by:

$$d_{hkl} = \frac{R_{hkl}}{L\lambda} \quad (7.1)$$

where L is called the camera length although it is not strictly related to any real length in the microscope. λ is the wavelength associated with the electrons for a given acceleration

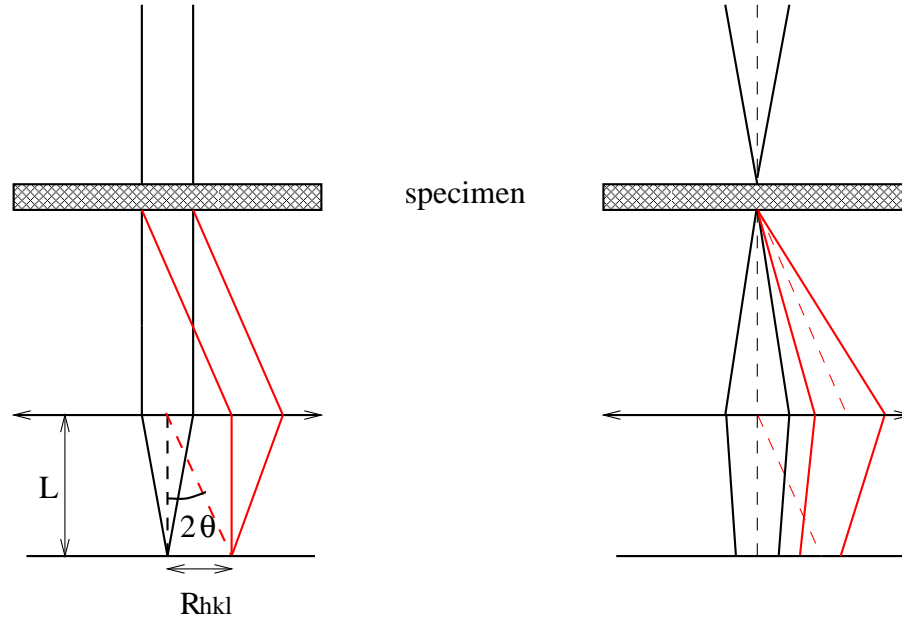


Figure 7.5: Schematic drawing of conventional diffraction pattern formation and convergent beam diffraction. In CBED, the points are replaced by discs which can contain supplementary structural information.

voltage, calculated with:

$$\lambda = \frac{12.26}{\sqrt{V(1 + 0.979 \cdot 10^{-6})}} \text{ \AA} \quad (7.2)$$

where V is the acceleration voltage and λ is given in Angströms. This formula account for relativistic corrections. The wavelength is 0.025 Å at 200 kV and 0.019 Å at 300 kV. For more accuracy, $L\lambda$ is often found by calibration with a gold thin foil. The following values were provided for 200 kV (JEOL 2000):

L, cm	$L\lambda$ measured, mm Å	$L\lambda$ theoretical
50	12.81	12.5
60	14.95	15
80	20.10	20
100	24.17	25
120	29.09	30
150	36.03	37.5
200	48.01	50

It can be noticed that these values are all less than 4% different from the theoretical ones.

It is possible to identify precipitates with conventional diffraction patterns, by trying to match against expected patterns. However, to distinguish $M_{23}C_6$ and M_6C for example,

which are both fcc (face centred cubic) and of similar lattice parameter, particular care is required (in this case, M_6C has a diamond-cubic structure for which reflections with h, k, l all even but $h + k + l \neq 4n$ are absent). The presence of the first order Laue zone (FOLZ) can also reveal features which help distinguish these carbides. Diffraction on its own is little appropriate to distinguish between different type of MX precipitates which all have a similar lattice parameter. On some replicas or foils, it is difficult to isolate one particular carbide because of the very small sizes. For this reason, CBED was used. In CBED, the incident electron beam is not parallel but convergent. This allows a reduction in probe size to a minimum of 10 nm, whereas it can hardly be less than 500 nm in conventional diffraction. Points are replaced by discs which contain information related to the space group of the precipitates. In fact, this space group can be determined from a suitable CBED pattern.

The systematic presence of Kikuchi's lines helps tilting of the specimen to a major zone axis. The CBED pattern (provided that it is not formed of blank disks) from a major zone axis can be related immediately to a particular precipitate with the help of reference.

However, to obtain a fine CBED pattern is time consuming and often, by the time the specimen had been oriented, the contamination blurs out the information in the discs.

ii Composition identification: EDX

In EDX or XEDS (X-ray energy dispersive spectrometry), the characteristic X-rays emitted by the different atoms as a consequence of their ionisation under the electron beam are used to identify them.

To perform EDX analysis in the TEM, the specimen was tilted to 45° ; the live time was 100 s. The dead time was kept below 20%.

EDX analysis was particularly useful on carbon replicas, where the precipitates are separated from the matrix. In thin foils, the size of most of the particles is so small that EDX patterns often contain an important contribution from the matrix. Most of the phases, once characterised by diffraction and composition, can be directly identified from their EDX pattern.